Available online at www.sciencedirect.com
SCIENCE DIRECT®

Dyes and Pigments 60 (2004) 103–110

DYES and PIGMENTS
www.elsevier.com/locate/dyepig

Photostability studies of thermomesomorphic derivatives of 2,5-dihydropyrrolo[3,4-c]pyrrole-1,4-dione

Serap Alp[a,*], Kadriye Ertekin[a], Matthias Horn[b,1], Sıddık Icli[c]

[a]Department of Chemistry, Faculty of Science and Arts, University of Dokuz Eylul, Buca, Izmir, Turkey
[b]Department of Chemistry & Biochemistry, University of California, Los Angeles 405 Hilgard Avenue, Los Angeles, CA 90095-1569, USA
[c]Institute of Solar Energy, University of Ege, 35100 Bornova, Izmir, Turkey

Received 9 May 2003; received in revised form 1 June 2003; accepted 12 July 2003

Abstract

In this study, the photophysical characteristics, like molar extinction coefficients, Stoke's shifts, quantum yields, radiative and fluorescence lifetimes, fluorescence rate constants, radiationless deactivation rate constants, and singlet energies of the fluorescent mesomorphic diketopyrrolopyrrole derivatives, (DPPDs), 3,6-bis(4-octyloxyphenyl)-2,5-dihydro-2,5-dimethylpyrrolo[3,4-c]pyrrole-1,4-dione (DPPD-1) and 3,6-bis(4′-butylbiphenyl-4-yl)-2,5-dihydro-2,5-dimethylpyrrolo[3,4-c]pyrrole-1,4-dione (DPPD-2) have been determined. The photostability studies were carried out under xenon arc lamp, direct and concentrated sunlight in solution of chloroform and tetrahydrofuran as well as in solid state, embedded in matrices of polyvinyl chloride (PVC) and sol-gel. The studies reveal that the photostabilities of the DPPD derivatives in PVC and sol-gel matrices are enhanced compared to solutions of chloroform and tetrahydrofuran.

Keywords: Diketopyrrolopyrroles; Fluorescence spectroscopy; Sol-gel matrix; Photostability studies

1. Introduction

In the last 20 years, aryl-derivatives of diketopyrrolopyrroles have been developed to industrially important red high performance pigments [1]. This organic chromophore has been intensely studied by chemists at Ciba [2–6] resulting in the commercialisation of products in various areas, e.g. for colouring of construction plastics, fibres and surface coatings such as automotive paints, prints and inks [7]. Their excellent properties such as high light fastness, very low solubility and extraordinary thermal stability are based on the formation of a 2-dimensional network by intermolecular hydrogen bonds (N···H···O) combined with Π – Π and van der Waals interactions of the aryl substituents between layers of molecules [8]. Detailed experimental and theoretical investigations on the influence of these forces have been done in order to gain and optimise solid state

---

* Corresponding author. Tel.: +90-232-453-5072/2255; fax: +90-232-453-4188.
E-mail address: serap.alp@deu.edu.tr (S. Alp).

[1] Present address: Institute for Thin Film Technology and Microsensorics e.V, Kantstrasse 55, 14513 Teltow, Germany.

0143-7208/$ - see front matter © 2003 Elsevier Ltd. All rights reserved.
doi:10.1016/S0143-7208(03)00143-8

parameters like crystal modification, particle size/surface and distribution control [9].

About a decade ago, besides heterocyclic pigments such as perylenes and quinacridones, this class of organic colorants, was also used outside of the conventional applications due to their functional properties like fluorescence and photoconduction. A number of electronic applications have been suggested for diketopyrrolopyrroles as charge generating materials for laser printers [10] and information storage systems [11]. In order to design novel photorefractive materials, the incorporation of the chromophoric DPPD derivatives into polymers was achieved first by Yu et al. [12].

Later, Tieke and co-workers realised two different series of DPPD-containing polymers, thus, aliphatic copolyesters and copolyurethanes [13], via their N-alkylated lactam groups, have been prepared as well as π-conjugated material by Suzuki coupling [14] towards electronic applications as OLED materials.

The chromophoric biheterocycle DPPD with a variable basic core structure was introduced into liquid crystal research by Praefcke and co-workers [15]. The essential feature of this anisotropic material is its N-alkylation in combination with aryl moieties in 3- and 6-position bearing long alkyl-chains. Variation of the substitution pattern and the length of alkyl-chains are versatile tools inducing different phase types [16]. Hence, even thermomesomorphic DPPD-containing polymers [17] and amphiphilic DPPD derivatives exhibiting lyotropic phase behaviour are known [18]. The interesting liquid crystalline and optical (even fluorescence) properties of DPPD-1 and DPPD-2 show that these materials are very promising towards advanced applications, e.g. organic voltaics [19]. This encouraged us to do further research regarding their photostability in different media with absorption and fluorescence emission based techniques.

The spectral data of molar extinction coefficients (ϵ), Stokes' shifts ($\Delta\lambda$), quantum yields (Q_f), radiative lifetimes (τ_o), fluorescence lifetimes (τ_f), the rate constants of fluorescence (k_f), the rate constants of radiationless deactivation (k_d) and singlet energies (E_s) of DPPD-1 and DPPD-2 were calculated. In order to clarify their photosensitivities, the short term and long-term photostabilities of DPPD derivatives were tested in solutions of $CHCl_3$ and THF and in solid matrices of PVC and sol-gel under xenon arc lamp and solar radiation.

2. Experimental

2.1. Materials

The polymer membrane components, polyvinyl chloride (PVC) (high molecular weight) and the plasticizer, bis-(2-ethylhexyl)phtalate (DOP), were obtained from Fluka and tetrahydrofuran (THF) was supplied from Aldrich.

The sol-gel components, tetraethyl orthosilicate (TEOS), and analytical grade concentrated hydrochloric acid were supplied from Merck. The surfactant additive triton X-100 (polyethylene glycol *t*-octylphenyl ether) was obtained from Merck. The absolute ethanol used throughout the study, was used without any further treatment. Other chemicals, nitric acid (HNO_3), hydrochloric acid (HCl) and chloroform ($CHCl_3$) were of analytical grade.

N-dodecyl perylenediimide [20] and *N*-abietyl perylenediimide were used as references for fluorescence quantum yield calculations of the DPPD derivatives.

The synthesis of DPPD-1 and DPPD-2 is published elsewhere [15]. Schematic structures of both molecules are shown in Fig. 1.

2.2. PVC membrane preparation process

The DPPD-doped membranes were composed according to the literature [21], containing 120 mg of PVC, 240 mg of plasticizer, 20 mmole of DPPD kg^{-1} polymer and 1.5 ml of dry THF. The resulting cocktails were spread onto a 125 μm polyester support (Mylar TM type) by using a spreading device (from Heidelberg, Germany). The polyester support is optically fully transparent, ion impermeable and exhibits good adhesion to PVC.

2.3. Sol-gel matrix and thin film preparation process

The DPPD doped silica gel glasses were prepared by hydrolysis of TEOS. 1 ml of 2 mM DPPD (in THF) was mixed with 1.5 ml of absolute ethanol in a glass vial and sonicated for 1 min. Afterwards, 1 ml of TEOS was added into the dye solution and sonicated for 5 min, followed by the addition of 1 ml of acidic water (pH = 2 via addition of HCl) and 20 μl of triton X-100 in order to improve the homogeneity of silica sol-gel and to give a crack-free monolith. In all cases, the solutions were aged at room temperature in closed glass vials [22].

Glass slides (11×40×1 mm) were used as solid support on which the sol-gel was coated by manual dip-coating technique. Prior to coating, the glass surface was activated by the treatment with concentrated HNO_3 for 24 h, then, washed with distilled water and ethanol. After evaporation of the solvents in a dessicator, the glass slides were fixed diagonally in a quartz sample cuvette in order to improve the reproducibility of the measurements. Film thickness of the glass slides was measured with a Tencor Alpha Step 500 Prophylometer and found to be 1.58 μm. This result was an average of eight measurements and exhibited a standard deviation of ±0.0066.

2.4. Instruments for spectroscopic measurements and solar radiation experiments

Absorption spectra of the DPPD derivatives in solutions, PVC coated Mylar films and sol-gel glass slides were measured with a Jasco V-530 UV–VIS spectrophotometer. The fluorescence emission spectra were recorded using a PTI-QM1 fluorescence spectrophotometer.

Concentrated solar radiation experiments were performed under Fix Focus FF 3.5 HTC GmbH (Germany) instrument. The instrument had a reflective surface area of 3.68 m^2, a usable reflector area of 2.66 m^2 and a focal length of 0.65 m^2. The inner side of the instrument was covered with a reflective aluminised polymer film. While an automatic photocell was focusing the sunlight on

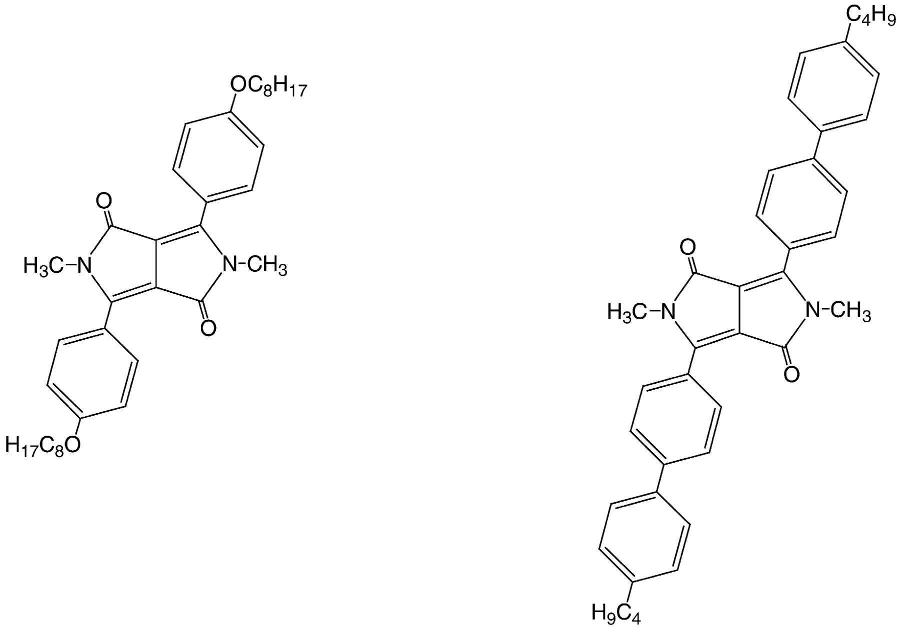

DPPD-1 **DPPD-2**

Fig. 1. Schematic structures of the DPPD-1 and DPPD-2.

X direction, manual focus was on *Y* direction (Fig. 2). The intensity of the concentrated sunlight was determined with a Vilbert Loumert radiometer at 312 nm radiation wavelength by comparison to direct sunlight (1 sun).

2.5. Molecular structure analysis

The synthesis of 3,6-bis(4-octyloxyphenyl)-2,5-dihydro - 2,5 - dimethylpyrrolo[3,4-c]pyrrole-1,4-dione (DPPD-1) and 3,6-bis(4′-butylbiphenyl-4-yl)-2,5-dihydro-2,5-dimethylpyrrolo[3,4-c]pyrrole-1,4-dione (DPPD-2) were carried out by using the earlier description [23].

DPPD-1: m.p. 105.7 °C. EA: (calculated: C, 75.49%; H, 8.45%; N, 4.89%; found: C 75.14% H 8.38% N 4.94%). F.W. $C_{36}H_{48}N_2O_4$ 572.79 g/mol.

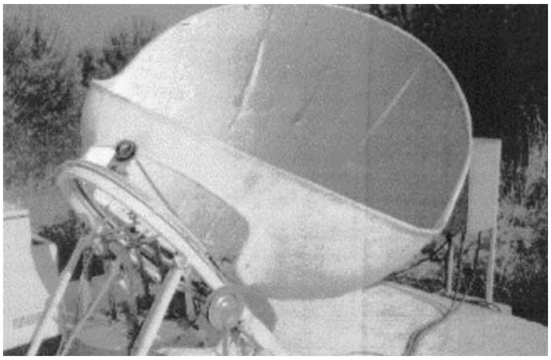

Fig. 2. Solar concentrator instrument at Ege University (FF 3.5-HTC GmbH, Germany).

MS (LR) *m/z* (%) = 573 (74) [$M^+ + 1$], 572 (100) [M^+], 347 (11), 81 (14), 69 (30), 57 (18), 43 (15).

IR (ATR): ν (cm^{-1}) = 2922, 2855 (C–H), 1699 (C=O), 1604 (aryl), 1511, 1473, 1431, 1371, 1264, 1185, 1087, 833.

^1H NMR: δ (ppm) 7.90/7.02 (arom. H, 8H, *J* = 9Hz), 4.03 (O-CH_2, 4H, *t*, *J* = 7Hz), 3.35 (N-CH_3, 6H, *s*), 1.81 (OCH_2CH_2, 4H, *tt*, *J* = 7 Hz), 1.52–1.23 (CH_2 groups, 20H, *m*), 0.90 CH_3, 6H, *t*, *J* = 7 Hz).

^{13}C NMR: δ (ppm) 162.66, 161.31, 147.68, 131.00, 120.23, 114.57, 107.97, 68.15, 29.30, 31.77, 29.45, 29.20, 29.09, 25.98, 22.62, 14.07.

DPPD-2: m.p. 219.0 °C. EA: (calculated: C, 82.73%; H, 6.94%; N, 4.82%; found: C, 81.85%; H, 6.85%; N, 4.84%). F.W. $C_{40}H_{40}N_2O_2$ 580.77 g/mol.

MS (LR) *m/z* (%) = 580 [M^+] (72), 375 (30) M^+–$C_{16}H_{13}$, 69 (100) $C_5H_9^+$, 57 (67), $C_4H_9^+$, 43 (65) $C_3H_7^+$.

IR (ATR): ν (cm^{-1}) = 2955, 2928, 2857 (C–H), 1671 (C=O), 1606, 1498, 1429, 1371, 1086, 1050, 817.

^1H NMR: δ (ppm) 7.99,7.75, 7.57, 7.29 (arom H, 16H, 4 *d*, *J* = 9 Hz), 3.41 (NCH_3, 6H, *s*), 2.68 (arom. H, 8H, *J* = 9 Hz), 1.66 (4H, *tt*, *J* = 7/7 Hz), 1.41 (4 h; *tt*, *J* = 7/7 Hz), 0.92 (CH_3, 6H, *t*, *J* = 7.5 Hz).

^{13}C NMR: δ (ppm) 162.60, 148.07, 143.75, 143.02, 137.12, 126.39, 126.39, 129.59, 128.99, 127.03, 126.92, 109.19, 35.32, 33.54, 22.39, 29.51, 13.95.

Table 1

Solvent	λ^{ab}_{max}	ϵ_{max}	λ^{f}_{max}	($\Delta\lambda$)	Q_f	τ_o	τ_f	k_f (10^9)	k_d	E_s
(a)										
$CHCl_3$	496	24,682	539	43	0.98	0.245	0.240	4.08	$8.33.10^7$	57.52
THF	497	26,955	535	38	0.95	0.232	0.220	4.31	$2.27.10^8$	57.40
PVC	500	24,698	534	34	0.49*	0.259	0.127	3.86	$4.02.10^9$	57.06
(b)										
$CHCl_3$	496	27,667	564	68	0.47	0.243	0.114	4.12	$4.65.10^9$	57.52
THF	500	34,864	558	58	0.56	0.203	0.114	4.93	$3.87.10^9$	57.06
PVC	505	27,680	559	54	0.65*	0.264	0.172	3.79	$2.04.10^9$	56.49
Sol-gel	496	27,715	550	54	–	0.302	–	3.31	–	57.52

(a) UV–Vis and emission spectroscopy data of DPPD-1 and (b) DPPD-2 in $CHCl_3$, THF and in solid matrices of PVC and sol-gel. λ^{ab}_{max}: absorption maximum (nm); λ^{f}_{max}: emission maximum (nm); ϵ_{max}: molar extinction coefficient (l mol^{-1} cm^{-1}) ; $\Delta\lambda$: Stokes' shifts (nm); Q_f: fluorescence quantum yield; τ_o: radiative lifetime (ns); τ_f: fluorescence lifetime (ns); k_f: rate constant of fluorescence (10^9 s^{-1}); k_d: rate constant of radiationless deactivation (s^{-1}) and E_s: singlet energy (kcal/mol).

3. Results and discussion

3.1. Matrix compatibility and spectral data

Samples of DPPD-1 and DPPD-2 were investigated in $CHCl_3$ and THF and in solid matrices of PVC and sol-gel. It should be noted that DPPD-2 was compatible with both of the solid matrices. However, studies of DPPD-1 could only be performed in PVC, due to the aggregate formation in sol-gel. This behaviour can be explained with the more lipophilic characteristic of DPPD-1 because of the presence of long octyloxy chains. Solutions of DPPD-1 and DPPD-2 were orange and greenish yellow, respectively, in $CHCl_3$ and THF. As expected, their colours did not show any change in PVC and sol-gel matrices even, the brightness of their colours was enhanced [24,25].

Table 1(a) summarises the absorption characteristics of DPPD-1. $\lambda_{max}(\epsilon)$: 496 (24,682) in $CHCl_3$, 497 (26,955) in THF and 500 (24,698) in PVC. Interestingly, the absorption maximum of DPPD-1 in PVC was found to shift to a longer wavelength compared to $CHCl_3$. This slight red shift was presumably due to the decrease of the polarity in the microenvironment of DPPD-1. In a similar way, DPPD-2 exhibited the following absorption characteristics: λ_{max} (ϵ): 496 (27,667) in $CHCl_3$, 500 (34,864) in THF and 505 (27,680) in PVC (Table 1(b)). As expected, the absorption maximum of DPPD-2 in sol-gel, λ_{max} (ϵ): 496 (27,715), was blue shifted with respect to THF and PVC, presumably because of the higher polarity in sol-gel matrix.

The emission spectra of DPPD-1 and DPPD-2 exhibited similar spectral shifts in different phases. The gathered absorption and emission spectra of

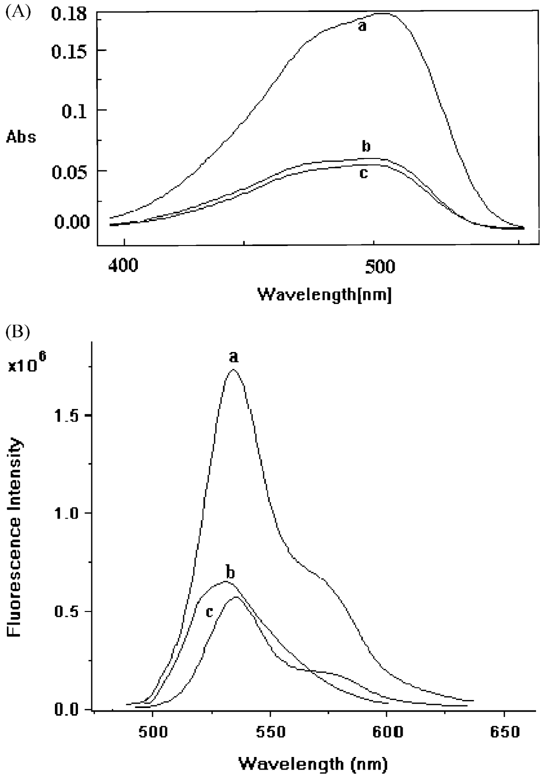

Fig. 3. (A) The absorption spectrum of DPPD-1: (a) PVC, $\lambda^{ab}_{max} = 500$ nm, (b) THF, $\lambda^{ab}_{max} = 497$ nm, (c) $CHCl_3$, $\lambda^{ab}_{max} = 496$ nm. (B) The emission spectrum of DPPD-1 in; (a) $CHCl_3$, $\lambda^{em}_{max} = 539$ nm, (b) PVC, $\lambda^{em}_{max} = 534$ nm, (c) THF, $\lambda^{em}_{max} = 535$ nm.

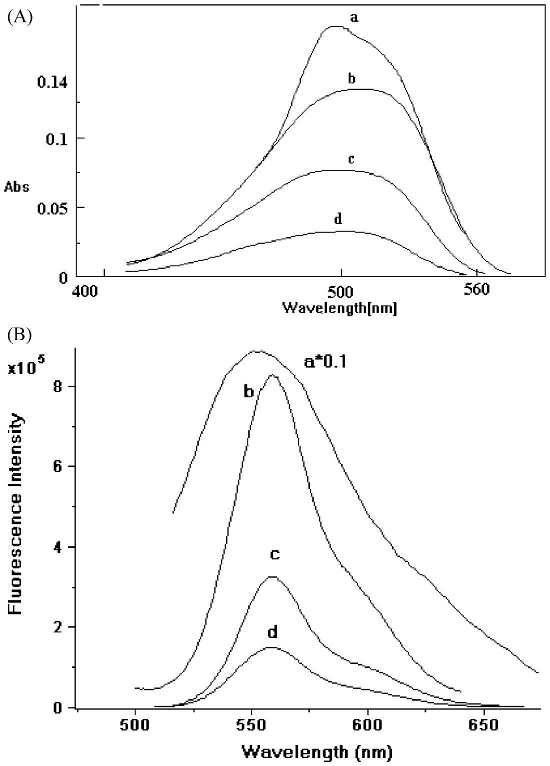

Fig. 4. (A) The absorption spectrum of DPPD-2: (a) sol-gel, $\lambda^{ab}_{max} = 496$ nm, (b) PVC, $\lambda^{ab}_{max} = 505$ nm, (c) THF, $\lambda^{ab}_{max} = 500$ nm, (d) $CHCl_3$, $\lambda^{ab}_{max} = 496$ nm. (B) The emission spectrum of DPP-2 in; (a) sol-gel, $\lambda^{em}_{max} = 550$ nm, (b) PVC, $\lambda^{em}_{max} = 559$ nm, (c) THF, $\lambda^{em}_{max} = 558$ nm, (d) $CHCl_3$, $\lambda^{em}_{max} = 564$ nm.

DPPD-1 and DPPD-2 were presented in Figs. 3 and 4, respectively.

Table 1(a) and (b) portrays that both of the compounds show the highest Stokes' shifts in $CHCl_3$. The Stokes' shift corresponds to the energy difference between the highest and the lowest singlet excited states. High Stokes' shift values indicate the occurrence of a large number of internal conversions at excited states. As a result, the higher Stokes' shifts in $CHCl_3$ can be explained with a high number of internal conversions with respect to the other microenvironments of DPPD derivatives.

The fluorescence quantum yields for DPPD-1 and DPPD-2 in $CHCl_3$ and THF were calculated with reference to absorption and fluorescence emission of *N*-dodecyl perylenediimide ($Q_f = 1$ in $CHCl_3$) [20]. Although *N*-dodecyl perylenediimide is a suitable reference in solution phase, it caused aggregate formation in solid matrices. Other well-known quantum yield standards, rose bengal, rhodamine 6G and eosin, were experimented in solid phase and all caused aggregate formation, excluding the *N*-abietyl derivative of perylenediimide. Therefore, *N*-abietyl perylenediimide was chosen as a reference for DPPD-1 and DPPD-2 doped PVC matrices. All of the references and DPPD derivatives were excited at 460 nm.

The quantum yields of DPPD-1 were found near unity in solution phases ($Q_f = 0.98$ in $CHCl_3$, $Q_f = 0.95$ in THF) whereas; DPPD-2 exhibited approximately 50% of Q_f value of DPPD-1 ($Q_f = 0.47$ in $CHCl_3$, $Q_f = 0.56$ in THF).

The quantum yield of *N*-abietyl perylenediimide in PVC matrix was calculated as $Q_f = 0.23$. With respect to the quantum yield of the reference, the values of DPPD derivatives were rather high ($Q_f = 0.49$ for DPPD-1 and $Q_f = 0.65$ for DPPD-2 in PVC matrix). These Q_f values would be evaluated in a different category, due to the usage of different references in solutions and solid phases. As a result, the fluorescence efficiencies of DPPD derivatives were enhanced in solid phases.

The fluorescence quantum yields of DPPD derivatives in PVC matrix were pointed out with a star (*) in Table 1(a) and (b), respectively.

The radiative lifetimes were calculated by the formula: $\tau_o = 3.5 \times 10^8 / \nu_{max}^2 \epsilon_{max} \Delta\nu_{1/2}$, where ν_{max} is the wave number in cm^{-1}, ϵ_{max} the molar extinction coefficient at the selected absorption wavelength, and $\Delta\nu_{1/2}$ denotes the half width of the selected absorption band in cm^{-1} [24,25]. Fluorescence lifetimes are estimated as $\tau_f = \tau_o Q_f$, the rate constants of fluorescence as $k_f = 1/\tau_o$ and the rate constants of radiationless deactivation as $k_d = (k_f/Q_f) - k_f$. Singlet energies (E_s) were extracted from the spectral data presented in Table 1(a) and (b).

3.2. Photostability test results

The photostabilities of DPPD derivatives were tested and evaluated in $CHCl_3$ and THF and in solid matrices of PVC and sol-gel under xenon arc lamp, solar and concentrated solar radiation. Using the xenon arc lamp, photostability tests of DPPD derivatives were carried out with a steady-state spectrofluorimeter in the mode of "Time Based Measurements". All of the fluorophores were excited at 460 nm and the data were acquired at their maximum emission wavelengths during one hour of monitoring. The acquired data of DPPD-2 are shown in Fig. 5, which reveals the excellent photostability in sol-gel but lower photostability in $CHCl_3$ and THF. The results of DPPD-1 were similar to the results of DPPD-2. Additionally, DPPD-1 and DPPD-2 exhibited an excellent photostability in PVC matrix. The long-term photostabilities of both derivatives in PVC were tested during eight consecutive months and found nearly the same with an intensity loss of only 1%.

The decreasing emission lines of DPPD-2 in $CHCl_3$ and THF shown in Fig. 5 would be because of the presence of photo-fading. In order to understand whether there had been photo-fading; the DPPD derivatives were exposed to the light at their absorption maxima in $CHCl_3$ and THF. These experiments were carried out with a steady-state UV–Vis spectrophotometer in the mode of "Time Based Measurements". The absorbance values, which acquired at every 5 s for 3 h, were exhibited parallel lines to the *x*-axis with the slopes of 1.93×10^{-7} (DPPD-1 in $CHCl_3$), 8.34×10^{-8} (DPPD-1 in THF), 1.91×10^{-7} (DPPD-2 in $CHCl_3$) and 2.44×10^{-7} (DPPD-2 in THF). As a result, this study has proved that there was no photo-fading behaviour of DPPD derivatives in

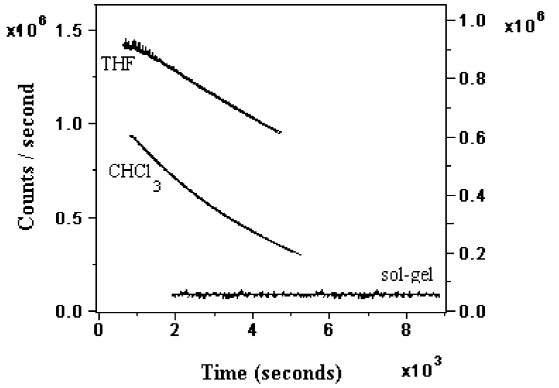

Fig. 5. Photostability test results of DPPD-2 in THF, $CHCl_3$ and sol-gel matrix; after exposure to xenon-arc lamp for 1 h of monitoring.

solution phases. As mentioned above, the decrease of the emission intensities of DPPDs was related to dye-solvent interactions in excited states. On the other hand, the excellent photostability in sol-gel and PVC matrices would be related to the molecular rigidity of the immobilized DPPD derivatives.

3.3. Irradiation studies under direct and concentrated sunlight

Under direct sunlight, during effective hours of the day, fluorescence intensities of DPPD-1 and DPPD-2 in $CHCl_3$ and THF were measured after 1 h of irradiation periods. Throughout 6 h, gradual decreases were observed in fluorescence intensities of the DPPD derivatives which were similar to the results of xenon arc lamp irradiation studies. However, fluorescence intensities of PVC doped DPPD-1 and PVC and sol-gel doped DPPD-2 did not change after exposure to direct sunlight for 6 h, which was a proof of their excellent photostabilities in solid matrices.

In the next step, the photostabilities of DPPD derivatives were evaluated under concentrated sunlight by using a Fix Focus FF 3.5 HTC instrument. These studies were performed under 60 and 100 sun of concentrated sunlight in a water-cooled system. Decreases in emission intensities of DPPD-2 derivative under 60 and 100 sun of concentrated sunlight in $CHCl_3$, THF, PVC and sol-gel are shown in Fig. 6. After 20 min of irradiation under 60 sun, the fluorescence intensities dropped dramatically in $CHCl_3$, THF and PVC. When the same experiments were repeated on another day under 100 sun, parallel results were obtained. The sol-gel doped derivative did not show any significant emission signal change under the irradiation of 60 sun, but a 42% intensity decrease was observed under 100 sun.

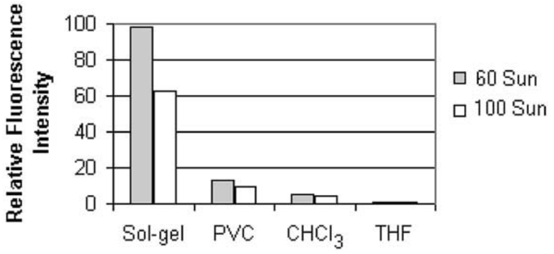

Fig. 6. Photostability test results of DPPD-2 in four different media; after 20 min exposure to 60 and 100 sun concentrated solar radiation. (Bars indicate the percentage of non-degraded parts of the DPPD-2 in sol-gel, PVC, $CHCl_3$ and THF.)

The withstanding of the sol-gel doped DPPD-2 even under the irradiation of 100 sun, can be concluded as a proof of its high photostability in sol-gel matrix. It should be noted that, under the direct solar radiation, photostabilities of DPPD-1 and DPPD-2 in solid matrices are satisfactory compared to the solution phase.

4. Conclusion

We have demonstrated that, the quantum yields of DPPD-1 were found near unity in $CHCl_3$ and THF, whereas, DPPD-2 exhibited approximately half the Q_f value of DPPD-1. As a result, DPPD-1 is a stronger fluorophore than the DPPD-2 in the solution phase. On the other hand, the quantum yields of DPPD-1 and DPPD-2 in the PVC matrix are determined as two fold of the quantum yield of the reference.

The photostability test results reveal that the fluorescence intensities of DPPD derivatives in $CHCl_3$ and THF gradually decreased under all types of light sources because of dye-solvent interactions in excited states. It has been experimentally proved that the decreasing of the photostability is not due to the photo-fading of the dye.

In contrast to the solution phase results, the sol-gel matrix compatible DPPD-2 did not show any considerable signal change under all types of light sources even after exposure to 100 sun of concentrated sunlight irradiation, which would be accepted as a proof of its high photostability.

It can be concluded that photostabilities of the solid phase doped DPPD-1 and DPPD-2 gives enough satisfaction for using in electronic devices such as OLED materials and many sun related applications.

References

[1] Wallquist O, Lenz R. Twenty years of DPP pigments—future perspectives. Macromol Symp 2002;187:617–29.

[2] Iqbal A, Cassar L. (to CIBA-GEIGY Corp.), US Patent, 4,415,685 (Nov, 15, 1983).

[3] Rochat AC, Cassar L, Iqbal A. (to CIBA-GEIGY Corp.), Europe Patent 9 4911 (Nov, 23,1983).

[4] Pfenninger J, Iqbal A, Rochat AC. (to CIBA-GEIGY Corp.), Europe Patent Application 184–981 (June 18,1986).

[5] Pfenninger J, Iqbal A, Rochat AC, Wallquist O. (to CIBA-GEIGY Corp.), Europe Patent Application 184-982 (June 18, 1986).

[6] Iqbal A, Pfenninger J, Rochat AC, Babler F. (to CIBA-GEIGY Corp.), Europe Patent Application 181–290 (May 4, 1986).

[7] Iqbal A, Cassar L, Rochat AC, Pfenninger J. New heterocyclic pigments. J Coat Tech 1988;60:37–45.

[8] Iqbal A, Jost M, Kirchmayr R, Pfenninger J, Rochat AC, Wallquist O. Bull the synthesis and properties of 1,4-diketo-pyrrolo[3,4-c]pyrroles. Soc Chim Belg 1988;97:615–43.

[9] Hao Z, Iqbal A. Some aspects of organic pigments. Chem Soc Rev 1997;26:203–13.

[10] Rochat AC, Wallquist O, Iqbal A, Mizuguchi J. (to CIBA-GEIGY Corp.), Europe Patent Application 0353184-A (1990).

[11] Mizuguchi J, Rochat AC. Information storage system based on 1,4-dithioketo-3,6-diphenyl-pyrrolo[3,4-c]-pyrrole. J Imag Technol 1991;17:123–6.

[12] Chan WK, Chen Y, Peng Z, Yu L. Rational designs of multifunctional polymers. J Am Chem Soc 1993;115: 11735–43.

[13] Lange G, Tieke B. New deeply coloured and fluorescent polymers with 1,4-dioxo-3,6-diphenylpyrrolo[3,4-c]pyrrole units in the main chain. Macromol Chem Phys 1999;200: 106–12.

[14] Beyerlein T, Tieke B. New photoluminescent conjugated polymers with 1,4-dioxo-3,6-diphenylpyrrolo[3,4-c]pyrrole (DPP) and 1,4-phenylene units in the main chain. Macromol Rapid Commun 2000;21:182–9.

[15] Praefcke K, Jachmann M, Blunk D, Horn M. Novel family of liquid crystals based on a known biheterocyclic pigment material: mesomorphic derivatives of 2,5-dihydropyrrolo[3,4-c]pyrrole-1,4-dione. Liq Cryst 1998;24: 153–6.

[16] Horn M. Flüssigkristalline pyrrolopyrrol-derivate. Berlin: Blunk-Verlag; 1999.

[17] Horn M, Hepuzer Y, Yagci Y, Eran BB, Cernenco U, Harabagiu V, et al. Synthesis and characterisation of thermomesomorphic polysiloxanes with 2,5-dihydropyrrolo[3,4-c]pyrrole-1,4-dione units in the main chain. Europ Polym J 2002;38:2197–205.

[18] Behnke M, Tieke B. Photoluminescent amphiphilic 1,4-diketo-3,6-diphenylpyrrolo[3,4-c]-pyrrole derivative and its complexes with polyelectrolytes. Langmuis 2002;18: 3815–21.

[19] Schmidt-Mende L, Fechtenkötter A, Müllen K, Moons E, Friend RH, MacKenzie JD. Self-organized discotic liquid crystals for high-efficency organic photovoltaics. Nature 2001;293:1119–22.

[20] Icil H, Icli S, Sayil C. Synthesis and properties of a new photostable soluble perylene dye: *N*,*N*′-di-(1-dehydroabietyl) perylene-3,4,9,10-bis(dicarboximide). Spectroscopy Lett 1998;31(8):1643–7.

[21] Seiler K, Simon W. Ion-selective optode membranes. Anal Chim Acta 1992;266:73–87.

[22] Fielding AJ, Davis CC, Brinker CJ, Scherer GW. Sol-gel science; the physics and chemistry of sol-gel processing. New York: Academic Press; 1986.

[23] Potrawa T, Langhals H. Fluoreszenzfarbstoffe mit großen Stokes Shifts—lösliche Dihydropyrrolopyrroldione. Chem Ber 1987;129:1075–8.

[24] Ertekin K, Alp S, Karapire C, Yenigul B, Henden E, Icli S. Fluorescence emission studies of an azlactone derivative embedded in polymer films: an optical sensor for pH measurements. J Photochem Photobiol A: Chem 2000; 137:155–61.

[25] Ertekin K, Karapire C, Alp S, Yenigul B, Icli S. Photophysical and photochemical characteristics of an azlactone dye in sol-gel matrix; a new fluorescent pH indicator. Dyes & Pigments 2003;56:125–33.